

EVALUATION OF THE IMPACT OF POWER SECTOR REFORM ON THE NIGERIA POWER SYSTEM TRANSIENT STABILITY

F. I. Izuegbunam*
Department of Electrical & Electronic
Engineering, Federal University of
Technology, Imo State,
NIGERIA.

E. N. C. Okafor
Department of Electrical and
Electronic Engineering, Federal
University of Technology, Imo State,
NIGERIA.

S. O. E. Ogbogu
Department of Electrical and
Electronic Engineering, Federal
University of Technology, Imo State,
NIGERIA.

ABSTRACT

This paper evaluates the impact of power sector reform on the Nigeria 330KV Grid System's response to large disturbances. The power sector reform on-going in Nigeria has the prospect of impacting positively to the transient stability status of the Nigeria Power system owing to massive investment in generation, transmission and distribution segments of the power sector. Evaluation of the transient stability status of pre-reform 8-plants, 26-bus system and projected 16-plants, 49-bus system under superimposed large disturbances were conducted using MATLAB program. The areas of instability threats in the existing network was highlighted, while the expected level of reform-induced improvement were identified; and recommendations made for further improvement on the system stability.

Keywords: Transient stability, existing network, projected network, swing curve, line losses

INTRODUCTION

The on-going reform in the Nigeria Power System have made this sector investment destination for interested investors, and have led to rapid expansion of the sector in terms of generation capacity, transmission links, and more new substations. The pre-reform Grid comprising of 8 plants, 26 bus-bars was highly vulnerable to transient instability owing to the network configuration with only one major loop linking buses 13-16-18-13. But the expansion in the nearest future based on the on-going construction works in both power generation and transmission facilities are expected to create more loops and provide better network configuration. The MATLAB Simulation of the transient stability analysis of the existing 330KV Grid System and the projected 16 plants, 49 bus-bars, 330KV Grid System showed a remarkable improvement in the System's ability to withstand large disturbances as well as power evacuation capability. Power system stability concerns the power system's response to disturbances [1], and a disturbance is a sudden change in an operating condition or operating parameters of the power system [2]. The power system is considered to operate at steady state when the operating parameters are assumed constant for the purpose of analysis. Under this condition, the peak-to-peak amplitude of the system current waveform is assumed time invariant (constant) [3]. The occurrence of a disturbance in a power system initially operating at steady state raises concern of whether an acceptable steady state condition could be reached as a consequence of the transient. When the disturbance is considered large, the stability concern is referred to as 'transient stability', which is the ability of the power system to maintain synchronism when subjected to severe transient disturbance. The resulting system response to such disturbance involves large excursions of generator rotor angle which is influenced by the non-linear power-angle relationship [4]. In carrying out transient stability studies, particularly in problems involving electromechanical transients, slow varying phase is assumed and justified due to high moments of inertia exhibited by turbine-generator sets [5]. The general purpose transient analysis involves quality investigation of the power system dynamic behavior [1]. The equations describing the dynamic behavior of a power system including the behavior of the synchronous generators in the system are highly nonlinear. In transient stability analysis, the generator parameters such as rotor angles, internal electromotive forces, terminal

*Corresponding Author: fabizu2000@yahoo.com

voltages, currents, etc. are particularly of interest. These parameters in turn influence the behavior of other network parameters such as voltage at key buses, active and reactive power flow in transmission lines and so on. In this paper, first swing stability is considered, hence the operation of various stability controllers are neglected since their responses are slow compared to relay operations speed. Figures 1 and 2 shows the existing 8 machines, 26 bus, 330KV Nigeria power system and projected 16 machines, 49-bus 330KV network respectively.

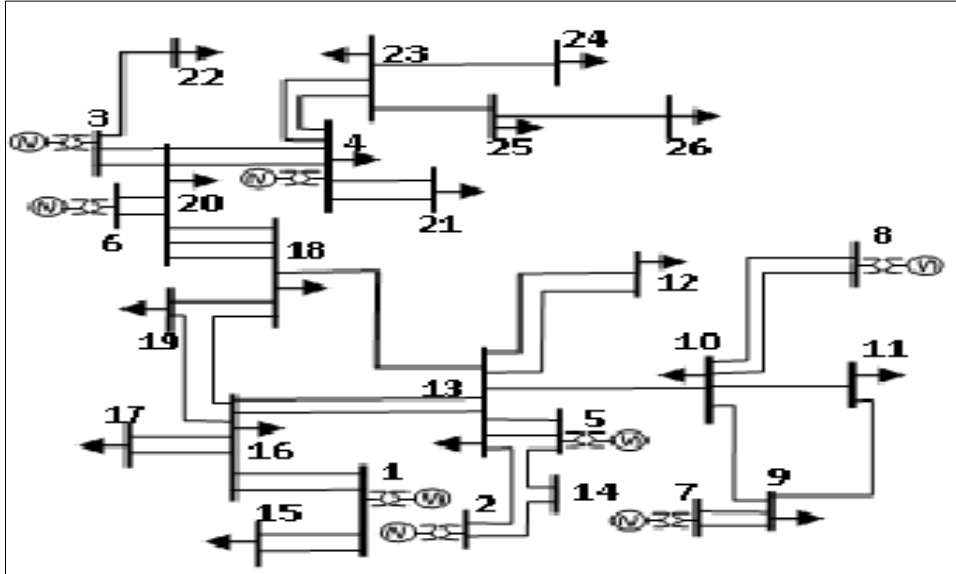


Figure 1: Pre-Reform (Existing) 330KV Nigeria grid

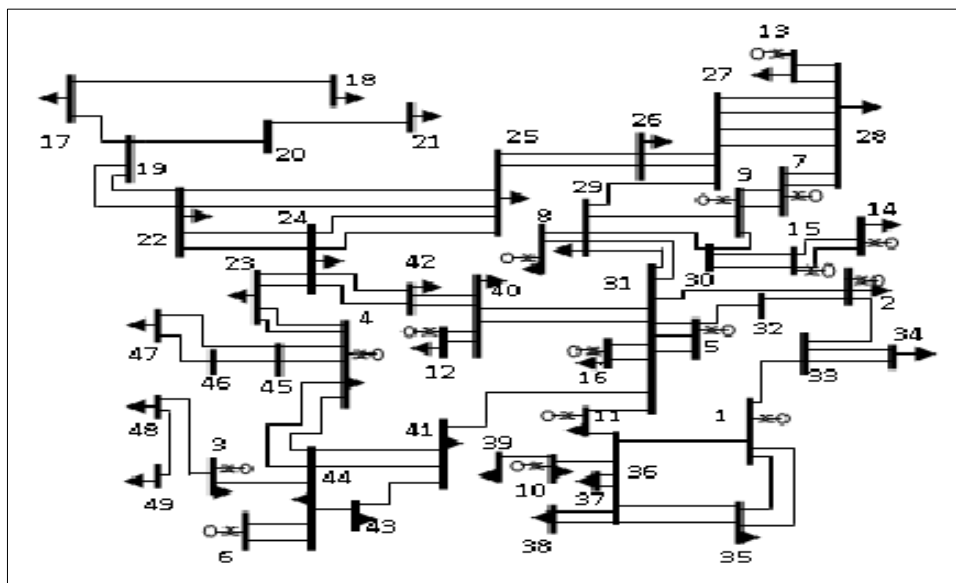


Figure 2: Projected 330KV Nigeria grid system [3]

THE UNIFIED POWER FLOW EQUATION

The active and reactive power for unified power flow equations are given as,

$$P_{ij} = (a_{ij} V_i)^2 g_{ij} - (a_{ij} V_i)(a_{ij} V_j) g_{ij} \cos(\theta_{ij} + \varphi_{ij} - \varphi_{ji}) - (a_{ij} V_i)(a_{ji} V_j) b_{ij} \sin(\theta_{ij} + \varphi_{ij} - \varphi_{ji}) \quad (1)$$

$$Q_{ij} = (a_{ij} V_i)^2 (b_{ij} + b_{ij}^{sh}) + (a_{ij} V_i)(a_{ji} V_j) b_{ij} \cos(\theta_{ij} + \varphi_{ij} - \varphi_{ji})$$

$$-(a_{ij} V_i)(a_{ji} V_j) g_{ij} \sin(\theta_{ij} + \varphi_{ij} - \varphi_{ji}) \quad (2)$$

The following substitutions are made for transmission lines, in-phase transformers and phase-shifting transformers respectively in equations (1) and (2):

(a) For transmission lines, $a_{ij} = a_{ji} = 1$, and $\varphi_{ij} = \varphi_{ji} = 0$; (b) For in-phase transformers,

$y_{ij}^{sh} = y_{ji}^{sh} = 0$, $a_{ji} = 1$, and $\varphi_{ij} = \varphi_{ji} = 0$; (c) For a phase-shifting transformers,

$y_{ij}^{sh} = y_{ji}^{sh} = 0$, $a_{ij} = 1$, and $\varphi_{ji} = 0$

Power flow by Newton-Raphson Method

The power flow solution of the network was provided using the Newton-Raphson technique which is found to be more efficient and practical. The method is adjudged mathematically superior to Gauss-Seidel technique due to its quadratic convergence [6].

MULTI-MACHINE POWER SYSTEM MODELING

The model considers the following assumptions [7], [8]:

1. The mechanical power input to each synchronous machine is constant.
2. Damping or asynchronous power is negligible.
3. The synchronous machines are represented electrically by constant voltage behind transient reactance models.
4. The motion of each synchronous machine rotor (relative to a synchronously rotating reference frame) is at a fixed angle relative to the angle of the voltage behind the transient reactance.
5. Loads are represented by constant impedances.

The constant voltage source $|E'| < \delta$ is determined from the initial conditions (that is, pre-disturbance power flow conditions). During the transient, the magnitude is held constant, while the variation of angle δ is governed by the swing equation [5]. The representation of the loads as constant impedances enable the elimination of algebraic network equations and hence reduce the system of equations for the multi-machine system consisting of only differential equations.

Mathematical Formulation

The electric power output of each existing grid machine as functions of the angular positions of other machines in the network is given as follows [3]:

$$P_1 = E_1^2 Y_{11} \cos \theta_{11} + E_1 E_2 Y_{12} \cos(\theta_{12} - \delta_1 + \delta_2) + E_1 E_3 Y_{13} \cos(\theta_{13} - \delta_1 + \delta_3) + E_1 E_4 Y_{14} \cos(\theta_{14} - \delta_1 + \delta_4) + E_1 E_5 Y_{15} \cos(\theta_{15} - \delta_1 + \delta_5) + E_1 E_6 Y_{16} \cos(\theta_{16} - \delta_1 + \delta_6) + E_1 E_7 Y_{17} \cos(\theta_{17} - \delta_1 + \delta_7) + E_1 E_8 Y_{18} \cos(\theta_{18} - \delta_1 + \delta_8)$$

$$P_2 = E_2^2 Y_{22} \cos \theta_{22} + E_2 E_1 Y_{21} \cos(\theta_{21} - \delta_2 + \delta_1) + E_2 E_3 Y_{23} \cos(\theta_{23} - \delta_2 + \delta_3) + E_2 E_4 Y_{24} \cos(\theta_{24} - \delta_2 + \delta_4) + E_2 E_5 Y_{25} \cos(\theta_{25} - \delta_2 + \delta_5) + E_2 E_6 Y_{26} \cos(\theta_{26} - \delta_2 + \delta_6) + E_2 E_7 Y_{27} \cos(\theta_{27} - \delta_2 + \delta_7) + E_2 E_8 Y_{28} \cos(\theta_{28} - \delta_2 + \delta_8) \quad (4)$$

⋮

$$P_n = E_n^2 Y_{nn} \cos \theta_{nn} + E_n E_1 Y_{n1} \cos(\theta_{n1} - \delta_n + \delta_1) + \dots + E_n E_{n-1} Y_{n,n-1} \cos(\theta_{n,n-1} - \delta_n + \delta_{n-1}) \quad (5)$$

The electric power output of each projected grid machine as functions of the angular positions of other machines in the network is given as follows [3]:

$$P_1 = E_1^2 Y_{11} \cos \theta_{11} + E_1 E_2 Y_{12} \cos(\theta_{12} - \delta_1 + \delta_2) + E_1 E_3 Y_{13} \cos(\theta_{13} - \delta_1 + \delta_3) + E_1 E_4 Y_{14} \cos(\theta_{14} - \delta_1 + \delta_4) + E_1 E_5 Y_{15} \cos(\theta_{15} - \delta_1 + \delta_5) + E_1 E_6 Y_{16} \cos(\theta_{16} - \delta_1 + \delta_6) + E_1 E_7 Y_{17} \cos(\theta_{17} - \delta_1 + \delta_7)$$

$$\begin{aligned}
& +E_1E_8Y_{18} \cos(\theta_{18} - \delta_1 + \delta_8) + E_1E_9Y_{19} \cos(\theta_{19} - \delta_1 + \delta_9) \\
& +E_1E_{10}Y_{1(10)} \cos(\theta_{1(10)} - \delta_1 + \delta_{10}) + E_1E_{11}Y_{1(11)} \cos(\theta_{1(11)} - \delta_1 + \delta_{11}) \\
& +E_1E_{12}Y_{1(12)} \cos(\theta_{1(12)} - \delta_1 + \delta_{12}) + E_1E_{13}Y_{1(13)} \cos(\theta_{1(13)} - \delta_1 + \delta_{13}) \\
& +E_1E_{14}Y_{1(14)} \cos(\theta_{1(14)} - \delta_1 + \delta_{14}) + E_1E_{15}Y_{1(15)} \cos(\theta_{1(15)} - \delta_1 + \delta_{15}) \\
& +E_1E_{16}Y_{1(16)} \cos(\theta_{1(16)} - \delta_1 + \delta_{16}) \tag{6}
\end{aligned}$$

$$\begin{aligned}
P_2 = & E_2^2Y_{22} \cos \theta_{22} + E_2E_1Y_{21} \cos(\theta_{21} - \delta_2 + \delta_1) + E_2E_3Y_{23} \cos(\theta_{23} - \delta_2 + \delta_3) \\
& +E_2E_4Y_{24} \cos(\theta_{24} - \delta_2 + \delta_4) + E_2E_5Y_{25} \cos(\theta_{25} - \delta_2 + \delta_5) \\
& +E_2E_6Y_{26} \cos(\theta_{26} - \delta_2 + \delta_6) + E_2E_7Y_{27} \cos(\theta_{27} - \delta_2 + \delta_7) \\
& +E_2E_8Y_{28} \cos(\theta_{28} - \delta_2 + \delta_8) + E_2E_9Y_{29} \cos(\theta_{29} - \delta_2 + \delta_9) \\
& +E_2E_{10}Y_{2(10)} \cos(\theta_{2(10)} - \delta_2 + \delta_{10}) + E_2E_{11}Y_{2(11)} \cos(\theta_{2(11)} - \delta_2 + \delta_{11}) \\
& +E_2E_{12}Y_{2(12)} \cos(\theta_{2(12)} - \delta_2 + \delta_{12}) + E_2E_{13}Y_{2(13)} \cos(\theta_{2(13)} - \delta_2 + \delta_{13}) \\
& +E_2E_{14}Y_{2(14)} \cos(\theta_{2(14)} - \delta_2 + \delta_{14}) + E_2E_{15}Y_{2(15)} \cos(\theta_{2(15)} - \delta_2 + \delta_{15}) \\
& +E_2E_{16}Y_{2(16)} \cos(\theta_{2(16)} - \delta_2 + \delta_{16}) \tag{7}
\end{aligned}$$

$$\begin{aligned}
P_n = & E_n^2Y_{nn} \cos \theta_{nn} + E_nE_1Y_{n1} \cos(\theta_{n1} - \delta_n + \delta_1) + \dots + E_nE_{n-1}Y_{2n-1} \cos(\theta_{nn-1} - \delta_n + \delta_{n-1}) \\
P_n = & \sum_{k=1}^n E_nE_kY_{nk} \cos(\theta_{nk} - \delta_n + \delta_k) \tag{8}
\end{aligned}$$

The rotor swing equations for the projected network generators are given as follows [3]:

$$\begin{aligned}
M_1\ddot{\delta}_1 = & P_{m1} - P_{e1} (\delta_1, \delta_2, \delta_3, \delta_4, \delta_5, \delta_6, \delta_7, \delta_8, \delta_9, \delta_{10}, \delta_{11}, \delta_{12}, \delta_{13}, \delta_{14}, \delta_{15}, \delta_{16}, \\
& \dot{\delta}_1, \dot{\delta}_2, \dot{\delta}_3, \dot{\delta}_4, \dot{\delta}_5, \dot{\delta}_6, \dot{\delta}_7, \dot{\delta}_8, \dot{\delta}_9, \dot{\delta}_{10}, \dot{\delta}_{11}, \dot{\delta}_{12}, \dot{\delta}_{13}, \dot{\delta}_{14}, \dot{\delta}_{15}, \dot{\delta}_{16}) \tag{9}
\end{aligned}$$

$$\begin{aligned}
M_2\ddot{\delta}_2 = & P_{m2} - P_{e2} (\delta_1, \delta_2, \delta_3, \delta_4, \delta_5, \delta_6, \delta_7, \delta_8, \delta_9, \delta_{10}, \delta_{11}, \delta_{12}, \delta_{13}, \delta_{14}, \delta_{15}, \delta_{16}, \\
& \dot{\delta}_1, \dot{\delta}_2, \dot{\delta}_3, \dot{\delta}_4, \dot{\delta}_5, \dot{\delta}_6, \dot{\delta}_7, \dot{\delta}_8, \dot{\delta}_9, \dot{\delta}_{10}, \dot{\delta}_{11}, \dot{\delta}_{12}, \dot{\delta}_{13}, \dot{\delta}_{14}, \dot{\delta}_{15}, \dot{\delta}_{16}) \tag{10}
\end{aligned}$$

⋮

$$M_n\ddot{\delta}_n = P_{mn} - P_{en} (\delta_1, \delta_2, \dots, \delta_{n-1}, \delta_n, \dot{\delta}_1, \dot{\delta}_2, \dots, \dot{\delta}_{n-1}, \dot{\delta}_n) \tag{11}$$

$$\text{Where, } \ddot{\delta} = \frac{d^2\delta}{dt^2}, \text{ and } \dot{\delta} = \frac{d\delta}{dt}$$

The rotor angular variations of n-generator bus system is determined by equation (9),

$$\Delta\delta_n = \Delta\delta_{n-1} + \frac{(\Delta t)^2}{M} P_{a(n-1)} \tag{12}$$

RESULTS AND DISCUSSION

The power flow result for existing 330KV Nigeria power system indicates flat voltage profile within acceptable limits in all the 26 buses. The voltage angles variations between buses are all below 25°, with the highest voltage angle of 26.612° occurring between Egbin and Afam, followed by 21.789° and 20.132° voltage angles deviations between Egbin and Alaoji, and Egbin and Gombe respectively. With reference to the steady-state stability limit of 90°, the system can be considered safe with no threat of disintegration in terms of static stability limit violation under the prevailing loading conditions. While the computed line losses stood at 119.662MW under the generators schedule and loading conditions. The losses in the lines 10-9, 10-8, 9-7 and 13-16 were quite significant (above 10MW) under this loading condition. Table 1 shows the lines with losses above 10MW in existing Network.

Projected Network Power Flow Result

The projected 330KV Nigeria power system power flow result indicates that 11 out of 49 buses experienced voltage magnitudes violation in excess of +10%, while the rest fall within acceptable limit. The vulnerable buses and their percentage voltage magnitudes violations include: bus 17 (Damaturu, 71.6%), bus 18 (Maiduguri, 80%), bus 19 (Gombe, 69.9%), bus 20 (Yola, 79.4%), bus 21 (Jalingo, 80.9%), bus 22 (Jos, 31.3%), bus 23 (Katempe, 14.4%), bus 24 (Gwagwa, 16.8%), bus 25 (Makurdi, 21.8%), bus 26 (Aliade, 19.6%), and bus 27 (New haven, 11%). This is shown in table 2. These buses have higher voltage magnitudes beyond acceptable limits due to reactive power build-up in between the transmission lines inter-connecting them, since the lines are comparatively long lines. For instance, Damaturu-Maiduguri, Gombe-Jos, Gombe-Yola and Yola-Jalingo lines are 308, 265, 217 and 132 kilometers in length respectively; and these cities are not industrialized to absorb excessive reactive power build up between the lines and the earth surface.

The computed line flow and losses of 421.953MW occurred in the network under the generation schedule and loading conditions considered. The losses in the following lines were quite significant: 19-22 (73.211MW), 11-36 (40.872MW), 7-28 (40.734MW), 24-23 (32.899MW), 22-24 (29.229MW), 11-31 (22.269MW), 26-27 (20.965MW), 4-23 (17.480MW), 24-42 (17.445MW), 1-35 (14.096MW), and 25-22 (12.875MW). This is shown in table 3. Table 4 shows generation schedule and load distribution used in the projected grid for evaluation, while table 5 gives the power flow result. The high line losses recorded along Gombe-Jos, Omotosho-Ikeja West single circuit lines and Afam-Ikot Ekpene, Gwagwa-Katempe and Jos- Gwagwa double circuit lines are indications of inadequate capacities of these lines to support anticipated level of power flow when all the new additional 8 generating plants become operational and tied to the grid. These transmission facilities requires expansion by converting the existing single circuit lines to double circuits as well as creating additional double circuit lines to reinforce the existing double circuit lines.

Results of Transient Stability Analysis of the Existing Network under Three-Phase Fault at Bus 16, Line 13-16

When a three-phase fault was superimposed at bus 16, line 13-16, the rotor angles swings of Afam and Okpai generators oscillate between 90° and above 100° , even at the clearing time of 0.16s. At a clearing time of 0.20s, the oscillating angles of the system generators increased beyond 120° as shown in figure 3. The system thus experienced instability at a clearing time of 0.22s as shown in figure 4. The critical clearing time for this fault condition is 0.21s, and the rotors swing curves at this time is shown in figure 5.

Results of Transient Stability Analysis of Projected Network under Three-Phase Fault at Bus 2, Line 2-31

When a three-phase fault was impressed at bus 2, line 2-31, figure 6 shows that Geregu generator experienced instability, while beyond the critical clearing time of 0.17s, generators (Shiroro and Omoku) became unstable in addition to generators (Geregu and Eyeen) which had earlier been lost due to instability occasioned by rotor acceleration of these generators at the instant of the initiated fault. At faulted bus 31, line 2-31, figure 7 indicates the loss of four generators (Shiroro, Geregu, Omoku and Eyeen) and beyond the critical clearing time of 0.29s, Okpai generator becomes unstable in addition to former.

Table 1: Lines with losses above 10MW in existing Network [3]

Bus No		Bus Name		Losses (MW)
From	To	From	To	
10	9	Ontisha	Alaoji	25.520
10	8	Ontisha	Okpai	20.970
9	7	Alaoji	Afam	17.109
13	16	Benin	Ikeja West	10.875

Table 2: Buses with intolerable voltage profile violation in projected Network [3]

Bus		Voltage profile (p.u)	% Violation
No	Name		
17	Damaturu	1.716	71.6%
18	Maiduguri	1.800	80%
19	Gombe	1.699	69.9%
20	Yola	1.794	79.4%
21	Jalingo	1.809	80.9%
22	Jos	1.313	31.3%
23	Katampe	1.144	14.4%
24	Gwagwa	1.168	16.8%
25	Makurdi	1.218	21.8%
26	Aliade	1.196	19.6%
27	New Haven	1.110	11.0%

Table 3: Lines with losses above 10MW] in projected Network [3]

Bus		Bus Name		Losses (MW)
From	To	From	To	
19	22	Gombe	Jos	73.211
11	36	Omosho	Ikeja West	40.872
7	28	Afam	Ikot ekpene	40.734
24	23	Gwagwa	Katampe	32.899
22	24	Jos	Gwagwa	29.229
11	31	Omosho	Benin	22.269
26	27	Aliade	New Haven	20.965
4	23	Shiroro	Katampe	17.480
24	42	Gwagwa	Lokoja	17.445
1	35	Egbin	Erukan	14.096
15	22	Makurdi	Jos	12.875

CONCLUSION

In this paper, accurate prediction of critical clearing time of 0.21s and establishment of stability margin of 0.238 for a three-phase fault at bus 16, line 13-16 of the existing grid was achieved using ode45 MATLAB programmed function. Beyond this critical clearing time, the system experienced total collapse due lack of proper looped structure. The network lines that experienced high losses required reinforcement and fortification. While the results of transient stability analysis of the projected 330KV Nigeria grid system showed better network configuration with improved looped structure. Though in the power flow simulation, some buses interconnected through long transmission lines experienced excessive voltage profile violations, and few other lines recorded high power losses. The network response to superimposed transients exposed some vulnerable plants which might require close monitoring and whose inertia could be improved upon. The paper also established the critical clearing time of 0.29s and stability margin of 0.448 for a three-phase fault impressed at bus 31, line 2-31; and provided vital technical information to guide the implementation of the on-going power sector reform for improved power system stability.

RECOMMENDATIONS

1. The high voltage profile violations at buses 17, 18, 19, 20, 21, 22, 23, etc, could be controlled by installing properly sized synchronous reactors in addition to strategically constructing substations to break very long transmission lines whereby the adjoining cities are not industrialized to absorb excess reactive power.
2. Line losses could be minimized by converting single circuit lines (19 – 22 and 11 – 36) to double circuit lines, and adding additional double circuit lines to reinforce the existing lines (7 – 28, 24 – 23, and 22 – 24).
3. Introduction of quick opening circuit breakers of high interrupting capacities (for instance CB with 3 cycle opening capability) will help stabilize the network during transients.
4. Improving on the inertia and reducing the reactance of instability prone generators can enhance system stability.

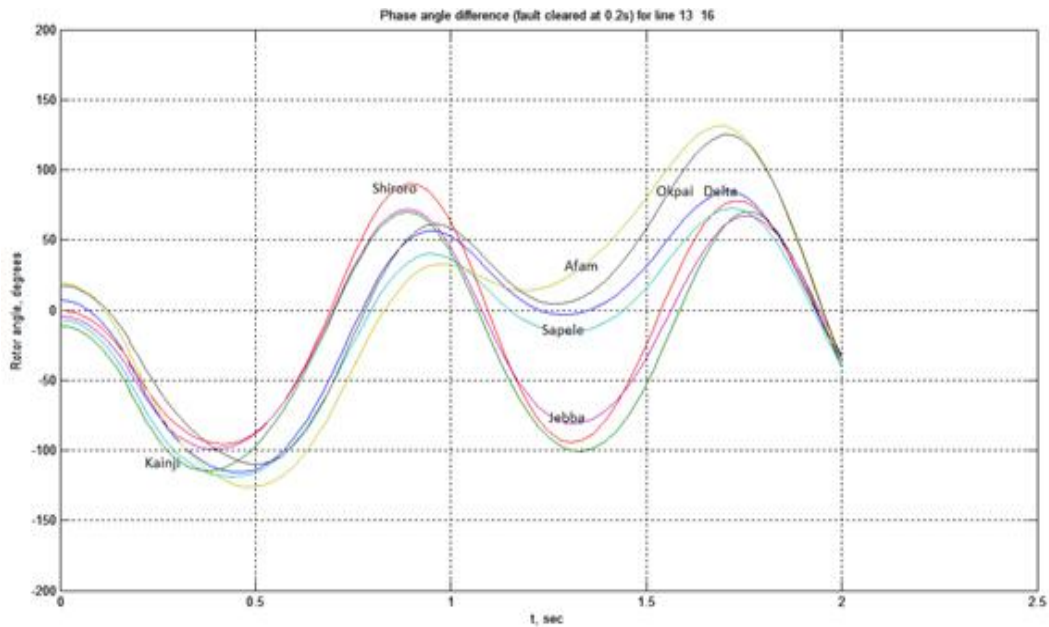


Figure 3: Swing curves for fault at bus 16, line 13 – 16 (Clearing Time: 0.20s)

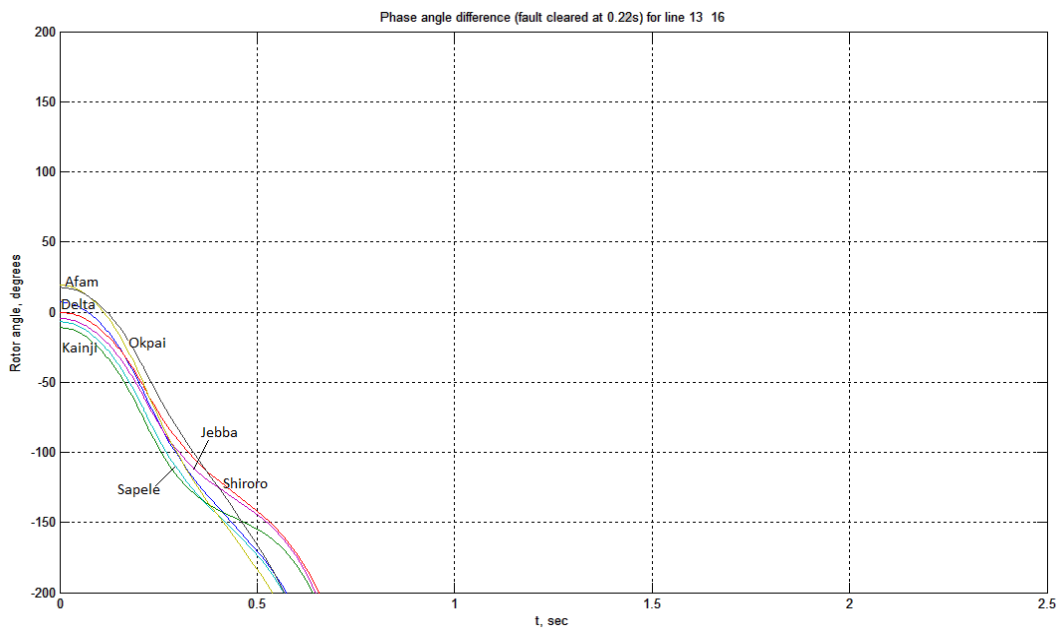


Figure 4: Swing curves for fault at bus 16, line 13 –16 (Clearing Time: 0.22s)

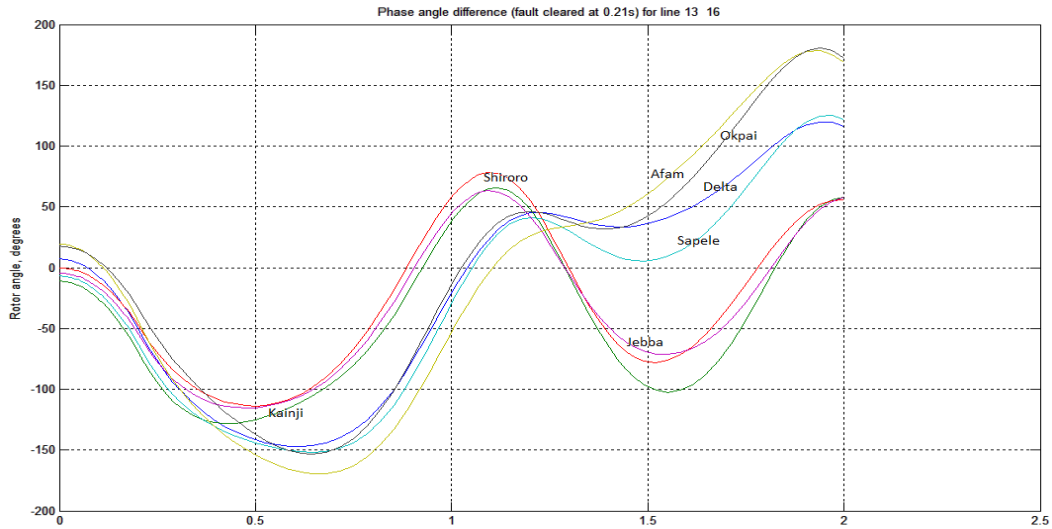


Figure 5: Swing curves for fault at bus 16, line 13 – 16(Critical clearing Time: 0.21s)

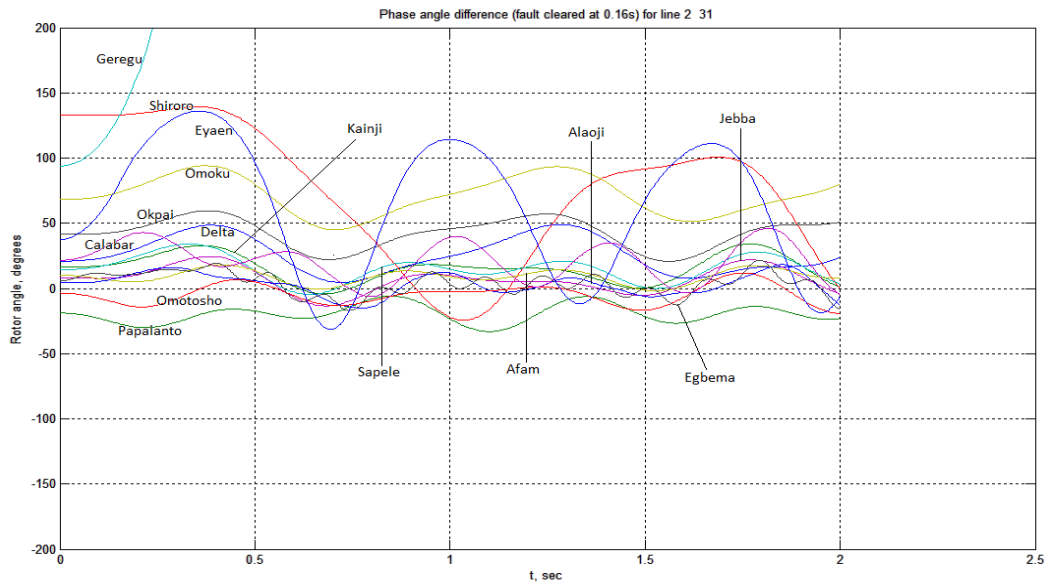


Figure 6: Swing curves for fault at bus 2, line 2 – 31(Clearing Time: 0.16s)

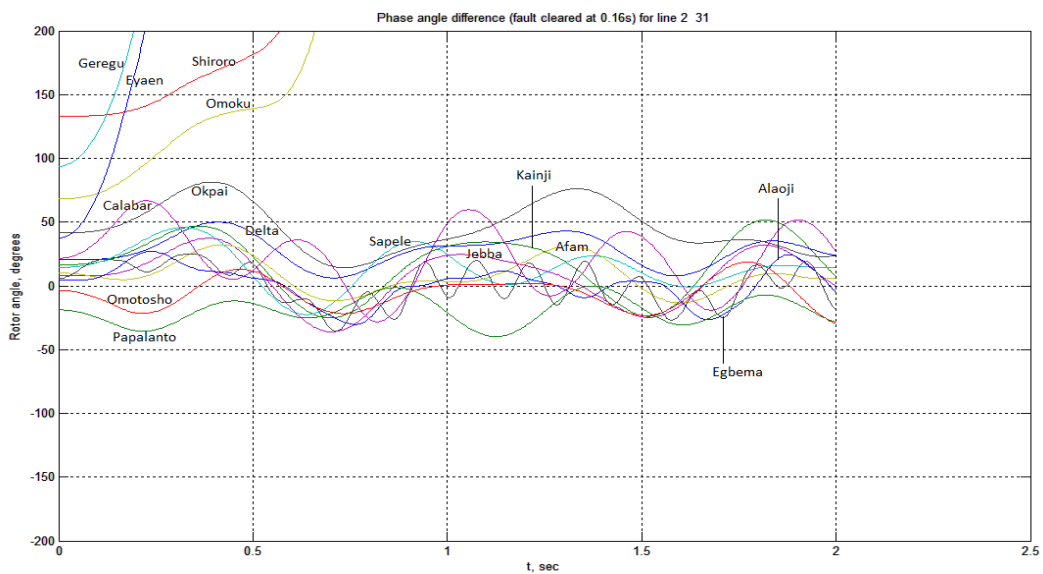


Figure 7: Swing curves for fault at bus 31, line 2 – 31(Clearing Time: 0.16s)

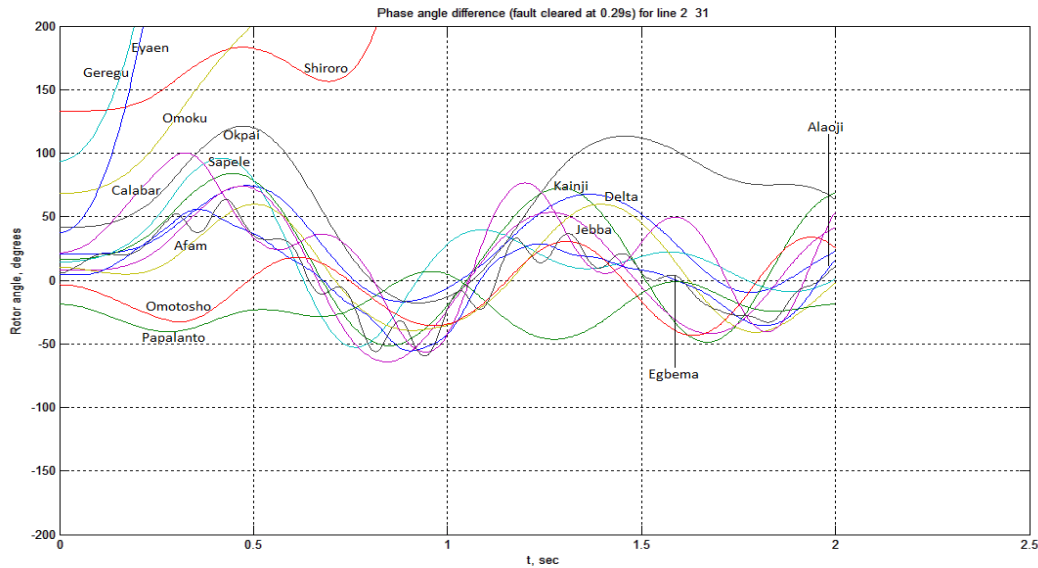


Figure 8: Swing curves for fault at bus 31, line 2 – 31 (Critical clearing Time: 0.29s)

REFERENCES

- [1] A. A. Fouad and V. Vittal, (1992). *Power System Transient Stability Analysis using the Transient Energy Function Method*. New Jersey: Prentice Hall Inc.
- [2] IEEE Task Force. (1982). Subcommittee of System Dynamic Performance, Power Systems Engineering Committee PES. Proposed Terms and Definitions for Power System Stability. *IEEE Transactions PAS-101*, pp 1894-1898.
- [3] F. I. Izuegbunam. (2010). *Transient Stability Analysis of Nigeria Power System: Multimachine Approach*. Ph.D Thesis, Federal University of Technology, Owerri, Nigeria,
- [4] P. Kundur. (1994). *Power System Stability and Control*. USA: McGraw Hill Inc.
- [5] A. R. Bergen and V. Vittal. (2000). *Power System Analysis, 2nd Edition*. New Jersey: Prentice Hall Inc.
- [6] H. Saadat. (2002). *Power System Analysis*. New Delhi: Tata McGraw Hill.
- [7] E.W. Kimbark. (1948). *Power System Stability*. Vol. 1: Synchronous Machine. New York: John Wiley & Sons.
- [8] P. M. Anderson and A. A. Fouad. (2002). *Power System Control and Stability*. Second Edition, Wiley: IEEE Press.

Table 4: Projected grid generation schedule and load distribution

Bus no	Bus code	V (pu)	Angle (Deg.)	P_load MW	Q_load Mvar	P_gen MW	Q_gen Mvar	Qmin Mvar	Qmax Mvar	Injected Mvar
1	1	1	0	0	0	1254	777	-550	800	0
2	2	1	0	0	0	682	423	-100	120	0
3	2	1	0	0	0	699	433	-250	300	0
4	2	1	0	200	123.9	600	372	-300	370	0
5	2	1	0	0	0	683	348	-280	340	0
6	2	1	0	19	11.8	303.5	376	-200	270	0
7	2	1	0	117	72.5	302	187	-150	200	0
8	2	1	0	0	0	536	332	-260	330	0
9	2	1	0	454	281.4	480	298	-250	290	0
10	2	1	0	0	0	326	202	-160	200	0
11	2	1	0	0	0	323	200	-160	200	0
12	2	1	0	0	0	444	275	-220	270	0
13	2	1	0	90	55.76	600	372	-280	370	0
14	2	1	0	0	0	240	149	-100	140	0
15	2	1	0	0	0	360	223	-180	220	0
16	2	1	0	0	0	480	298	-250	290	0
17	0	1	0	62	38	0	0	0	0	0
18	0	1	0	115	71	0	0	0	0	0
19	0	1	0	141	87	0	0	0	0	0
20	0	1	0	82	51	0	0	0	0	0
21	0	1	0	61	38	0	0	0	0	0
22	0	1	0	141	87	0	0	0	0	0
23	0	1	0	307	190	0	0	0	0	0
24	0	1	0	173	107	0	0	0	0	0
25	0	1	0	90	56	0	0	0	0	0
26	0	1	0	61	38	0	0	0	0	0
27	0	1	0	247	153	0	0	0	0	0
28	0	1	0	82	51	0	0	0	0	0
29	0	1	0	276	171	0	0	0	0	0
30	0	1	0	90	56	0	0	0	0	0
31	0	1	0	218	135	0	0	0	0	0
32	0	1	0	78	48	0	0	0	0	0
33	0	1	0	380	236	0	0	0	0	0
34	0	1	0	302	187	0	0	0	0	0
35	0	1	0	340	211	0	0	0	0	0
36	0	1	0	925	573	0	0	0	0	0
37	0	1	0	650	403	0	0	0	0	0
38	0	1	0	110	68	0	0	0	0	0
39	0	1	0	420	260	0	0	0	0	0
40	0	1	0	26	16	0	0	0	0	0
41	0	1	0	430	266	0	0	0	0	0
42	0	1	0	70	43	0	0	0	0	0
43	0	1	0	78	48	0	0	0	0	0
44	0	1	0	19	12	0	0	0	0	0
45	0	1	0	433	268	0	0	0	0	0
46	0	1	0	131	81	0	0	0	0	0
47	0	1	0	135.6	84	0	0	0	0	0
48	0	1	0	141	87	0	0	0	0	0
49	0	1	0	112	69	0	0	0	0	0

Table 5: Projected grid power flow result

Bus No.	Voltage Mag.(pu)	Angle (Degree)	Load Load	MW Mvar	Generated MW	Generated Mvar	Injected Mvar
1	1.000	0.000	400.000	247.900	1840.053	1694.541	0.000
2	1.010	23.771	0.000	0.000	682.000	-370.504	0.000
3	1.050	24.063	0.000	0.000	699.000	-425.568	0.000
4	1.050	17.216	200.000	123.900	600.000	-1775.149	0.000
5	1.020	22.966	0.000	0.000	683.000	415.426	0.000
6	1.050	21.769	19.000	11.800	303.500	-355.418	0.000
7	1.050	24.897	117.000	72.500	302.000	-919.643	0.000
8	1.050	24.500	0.000	0.000	536.000	-641.801	0.000
9	1.050	24.960	454.000	281.400	480.000	-105.417	0.000
10	0.960	-0.856	150.000	92.960	326.000	144.198	0.000
11	0.970	13.761	120.000	74.000	323.000	-140.745	0.000
12	1.050	19.137	0.000	0.000	444.000	-1476.315	0.000
13	1.050	23.023	90.000	55.760	600.000	-900.514	0.000
14	1.040	25.796	0.000	0.000	240.000	-816.762	0.000
15	1.050	25.538	0.000	0.000	360.000	492.467	0.000
16	1.010	22.511	0.000	0.000	480.000	-1101.969	0.000
17	1.716	8.442	62.000	38.000	0.000	0.000	0.000
18	1.800	7.418	115.000	71.000	480.000	0.000	0.000
19	1.699	8.626	141.000	87.000	0.000	0.000	0.000
20	1.794	7.585	82.000	51.000	0.000	0.000	0.000
21	1.809	7.382	61.000	38.000	0.000	0.000	0.000
22	1.313	13.986	141.000	87.000	0.000	0.000	0.000
23	1.144	16.767	307.000	190.000	0.000	0.000	0.000
24	1.168	15.838	173.000	107.000	0.000	0.000	0.000
25	1.218	16.624	90.000	56.000	0.000	0.000	0.000
26	1.196	17.502	61.000	38.000	0.000	0.000	0.000
27	1.110	20.740	247.000	153.000	0.000	0.000	0.000
28	1.075	21.994	82.000	51.000	0.000	0.000	0.000
29	1.049	23.692	276.000	171.000	0.000	0.000	0.000
30	1.052	25.082	90.000	56.000	0.000	0.000	0.000
31	1.012	22.396	218.000	135.000	0.000	0.000	0.000
32	1.015	23.224	78.000	48.000	0.000	0.000	0.000
33	0.987	-1.668	380.000	236.000	0.000	0.000	0.000
34	0.984	-1 864	302.000	187.000	0.000	0.000	0.000
35	0.970	-0.171	340.000	211.000	0.000	0.000	0.000
36	0.966	-0.436	925.000	573.000	0.000	0.000	0.000
37	0.938	-2.618	650.000	403.000	0.000	0.000	0.000
38	0.962	-0.901	110.000	68.000	0.000	0.000	0.000
39	0.942	-2.378	420.000	260.000	0.000	0.000	0.000
40	1.057	19.015	26.000	16.000	0.000	0.000	0.000
41	1.044	21.405	430.000	266.000	0.000	0.000	0.000
42	1.084	18.218	70.000	43.000	0.000	0.000	0.000
43	1.050	21.360	78.000	48.000	0.000	0.000	0.000
44	1.051	21.692	19.000	12.000	0.000	0.000	0.000
45	1.051	13.043	433.000	268.000	0.000	0.000	0.000
46	1.054	12.000	131.000	81.000	0.000	0.000	0.000
47	1.061	11.330	135.600	84.000	0.000	0.000	0.000
48	1.079	21.633	141.000	87.000	0.000	0.000	0.000
49	1.055	11.147	112.000	69.000	0.000	0.000	0.000
	TOTAL		8476.600	5249.220	8898.553	-6283.173	0.000